Power Converter Sizing for a Switched Doubly Fed Machine Propulsion Drive

Arijit Banerjee, *Student Member, IEEE*, Michael S. Tomovich, *Student Member, IEEE*, Steven B. Leeb, *Fellow, IEEE*, and James L. Kirtley, Jr., *Life Fellow, IEEE*

***Abstract*—Doubly fed machines (DFMs) can be used to make variable speed drives (VSDs) that not only provide full shaft speed control but also avoid the need for a dc electrical bus capable of providing full mechanical shaft power. This makes the DFM attractive for any VSD application where the primary power source is ac. Switching configuration of the DFM on-the-fly opens up opportunity to operate the DFM on a wider speed range with reduced power electronics. This paper explores the design requirements for a switched DFM rotor power electronics in full-speed-range VSD applications, including propulsion drives. Tradeoffs are examined for power electronics sizing versus transient settling characteristics.**

***Index Terms*—AC machines, drive design, electric vehicles, minimization, motor drives, power conversion.**

NOMENCLATURE

$v_{\rm dc}, v_{\rm PE}$	DC supply voltage and power electronics voltage rating [per unit (p.u.)].
i_s, i_r	Stator and rotor currents (referred to the stator) (p.u.).
r_s, r_r	Stator and rotor resistances (referred to the stator) (p.u.).
x_s, x_r, x_m	Stator, rotor (referred to the stator), and mutual inductances (p.u.).
τ	Electromagnetic torque (p.u.).
ω_B	Base frequency (same as ac supply frequency) (rad/s).
v_s, v_r	Stator and rotor voltages (referred to the stator) (p.u.).
ω_s, ω_e	Stator flux frequency and rotor speed (p.u.).
$\omega_T, \omega_{\rm max}$	Transition speed between modes and maximum speed (p.u.).
I_r	Rated rotor current (referred to the stator) (p.u.).
δ	Angle between stator flux and stator voltage (rad).
ψ_s	Stator flux (p.u.).
X_d, X_q	d- and q-axis components of X.
$X_{\rm dc}, X_{\rm ac}$	Corresponding dc mode and ac mode values of X.

Manuscript received February 25, 2014; accepted May 6, 2014. Date of publication June 10, 2014; date of current version January 16, 2015. Paper 2014-IDC-0119, presented at the 2013 IEEE International Electric Machines and Drives Conference, Chicago, IL, USA, May 12–15, and approved for publication in the IEEE TRANSACTIONS ON INDUSTRY APPLICATIONS by the Industrial Drives Committee of the IEEE Industry Applications Society. This work was supported in part by the Electric Ship Research and Development Consortium under the Office of Naval Research and in part by the Grainger Foundation.

The authors are with the Department of Electrical Engineering and Computer Science, Massachusetts Institute of Technology, Cambridge, MA 02139 USA (e-mail: arijit@mit.edu; tomovich@mit.edu; sbleeb@mit.edu; kirtley@mit.edu).

Color versions of one or more of the figures in this paper are available online at http://ieeexplore.ieee.org.

Digital Object Identifier 10.1109/TIA.2014.2330074

I. INTRODUCTION

DOUBLY fed machines (DFMs) have been predominantly used for applications with a limited speed range of operation such as in power generation in wind turbines and fly wheel energy storage [1], [2]. The major advantage of using a DFM for such applications, as opposed to a squirrel cage or a synchronous motor, is that it requires reduced power electronics capability. However, in applications where a wider speed range is desirable, as in propulsion, typical approaches to power electronics and source connection fail to reduce the power electronics requirement.

Operating DFMs in different configurations using multiple switches open up opportunity in achieving wider operating speed range with reduced power electronics. Denoting this group of DFM-based drives as "switched DFM," it typically has a controlled converter on the rotor, whereas the stator is connected to one or many sources through switches. Depending on the operating speed, the stator switch configurations are altered to ensure different operating modes of the DFM. For example, [3] reported a drive configuration in which, during low-speed operation, the stator is shorted, whereas during high-speed operation, the stator is connected to an ac source. Similar approaches have been used for developing and conceptualizing variable speed drives (VSDs) for hydroelectric power stations [4], ship propulsion [5], and centrifugal loads [6].

Unlike the configuration of shorting the stator, the switched DFM in [5] proposes to use a dc source excitation in low-speed operating mode. This leads to reduced structural noise at low operating speeds critical for ships intended for naval applications [7], [8]. The proposed drive, shown in Fig. 1, has two modes of operation: dc or low-speed mode and ac or high-speed mode. In dc mode, the stator of the DFM is connected to a dc supply, and the machine is equivalent to a wound field synchronous machine. In ac mode at higher shaft speeds, the stator of the DFM is connected to the ac supply. The rotor is driven by variable frequency power electronics in both modes. This arrangement can be controlled to operate the DFM drive in and through the two modes seamlessly [9].

While [3] apparently used an iterative method to choose a transition speed to minimize the rotor converter size, [5] and [6] used steady-state load torque-speed characteristic to determine the size of the controlled rotor converter. However, there are multiple design variables that need to be considered in order

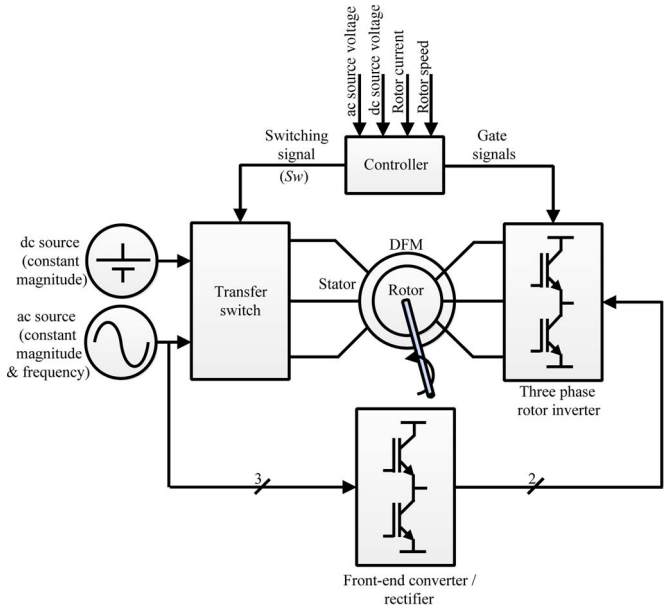

Fig. 1. Proposed configuration of a switched DFM drive enabling wide-speed-range operation with reduced power electronics.

to design a switched DFM drive. This paper presents a design procedure for the proposed switched DFM drive shown in Fig. 1 based on the requirement of a drive torque-speed capability. The design goal is to minimize rotor power electronics requirement while the DFM is operated on a full-speed range within rated conditions. The process will be illustrated using a demonstration DFM with practical machine parameters. The drive design includes the selection of different design variables such as the transition speed between the operating modes, dc mode stator voltage, rotor power electronics voltage and current rating, ac mode synchronous speed, maximum speed, and ac mode reactive power capability.

For a typical ship propulsion drive, the steady-state load torque requirement is proportional to the square of the shaft speed. Based on mechanical requirements, the maximum commandable shaft torque required in the "low-speed" region can be either the same as or lower than the rated drive torque in the "high-speed" mode. For the example design, the required low-speed torque capability for the drive is considered to be 75% of the high-speed torque capability.

II. DFM Drive Capability Analysis and Design

The rotor power converter sizing requirement is analyzed using a steady-state DFM model. Transient analysis is also performed to ensure that the designed drive operates seamlessly during mode transition. A steady-state DFM model in stator flux orientation can be derived ignoring the time-derivative terms in the machine model [9]. Using normalized variables and parameters with respect to base quantities, the machine can be described by

$$v_{sd} = r_s i_{sd} \tag{1}$$
$$v_{sq} = \omega_s \psi_s + r_s i_{sq} \tag{2}$$
$$v_{rd} = r_r i_{rd} - (\omega_s - \omega_e)\psi_{rq} \tag{3}$$
$$v_{rq} = r_r i_{rq} + (\omega_s - \omega_e)\psi_{rd} \tag{4}$$

whereas the normalized electromagnetic torque is governed by

$$\tau = -\frac{x_m}{x_s}\psi_s i_{rq} \tag{5}$$

and the normalized flux linkage equations are

$$\psi_s = x_s i_{sd} + x_m i_{rd} \tag{6}$$
$$0 = x_s i_{sq} + x_m i_{rq} \tag{7}$$
$$\psi_{rd} = x_r i_{rd} + x_m i_{sd} \tag{8}$$
$$\psi_{rq} = x_r i_{rq} + x_m i_{sq}. \tag{9}$$

The rotor quantities used in the model are referred to the stator. Therefore, to obtain actual rotor values, the turns ratio from the stator to the rotor must be considered. The ac source voltage and the rated stator current are considered to be base quantities and hence are unity in normalized form. The ac supply frequency is chosen as the base quantity for the stator flux frequency and the rotor speed. This makes normalized stator flux frequency ω_s zero in dc mode and unity in ac mode.

A. Rotor Power Electronics Requirement for an Ideal DFM

As a precursor, an analysis of an ideal DFM is considered to illustrate the benefit of the proposed drive in reducing power electronics requirement for full-speed-range operation. The impact of drive torque requirement on minimizing rotor power electronics is evaluated, which directly translates into the design choice of the mode transition speed and the maximum operating speed of the drive.

Assuming zero resistances, leakages, and negligible magnetizing current, the normalized rotor current rating (referred to the stator) is equal to the stator current rating of unity. Using (3), (4), and (6)–(9), the rotor voltage required is

$$v_r = |\omega_s - \omega_e|\psi_s. \tag{10}$$

The operating stator flux in ac mode is determined by the ac supply voltage and frequency and hence is always unity. For maximum utilization of the DFM, the rotor current rating of the DFM sets the current rating of the rotor power electronics. Unity rotor current and stator flux ensure that maximum torque capability of the DFM is utilized in ac mode.

The choice of stator flux in dc mode depends on the torque requirement in low-speed mode. For a unity torque requirement in low-speed mode, the rotor current and the stator flux must be maintained at unity. If dc mode stator flux is unity, then required rotor voltage is proportional to speed in dc mode and proportional to slip speed in ac mode, as shown in Fig. 2. As a concrete example, a transition at "A" from dc mode to ac mode will ensure operation of the drive from 0- to 1.5-p.u. speed while requiring a maximum rotor voltage of 0.5 p.u. (operating on OAEB path in Fig. 2).

If a lower electromagnetic drive torque capability is acceptable at low speed, for example, 75% to that at high speed, the stator flux in dc mode can be reduced to 0.75 p.u. while maintaining the rotor current at unity across the complete speed range. The reduction in stator flux in the dc mode directly

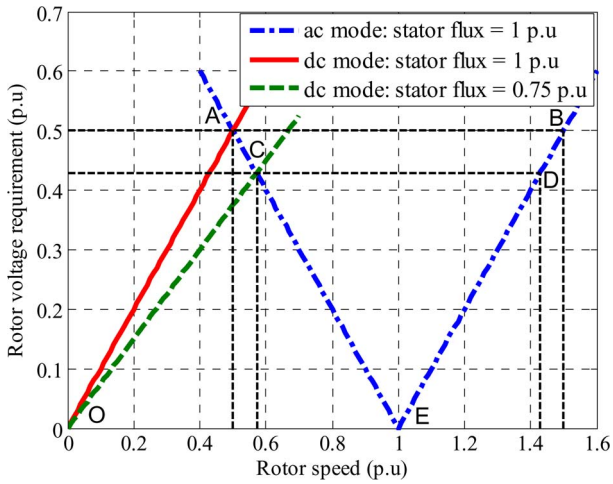

Fig. 2. Ideal DFM: rotor power electronics voltage rating of 0.5 p.u. can enable an operating speed range of 0–1.5 p.u. (OAEB), whereas a voltage rating of 0.43 p.u. enables an operating speed range of 0–1.43 p.u. (OCED).

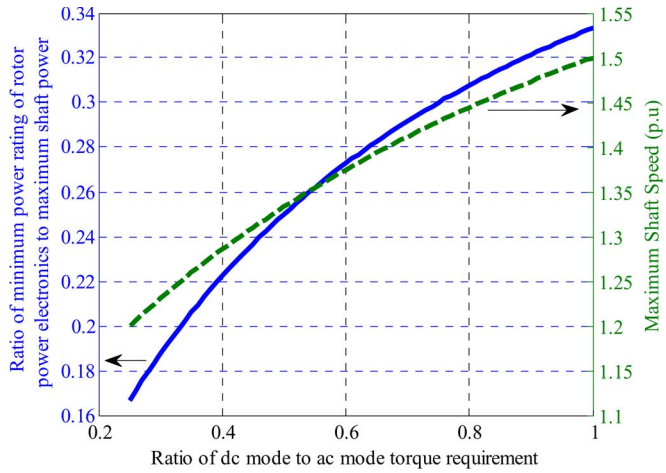

Fig. 3. Ideal DFM: lowering the requirement of the low-speed torque lowers rotor power electronics requirement and maximum shaft speed (for a designed ac supply frequency and number of pole pair).

impacts the required rotor voltage since the slope of the rotor voltage requirement curve in Fig. 2 is proportional to the stator flux. In this case, transitioning at "C" enables the drive to operate on a speed range from 0 to 1.43 p.u. while requiring a maximum rotor voltage of 0.43 p.u. (OCED path). In general, the transition speed that minimizes the maximum required rotor voltage can be computed equating required voltage in the dc and ac modes at the mode transition using (10), i.e.,

$$v_{\mathrm{rdc}}|_{\omega_T} = |-\omega_T|\psi_{\mathrm{sdc}} = |1-\omega_T| = v_{\mathrm{rac}}|_{\omega_T} = v_{\mathrm{PE}}. \quad (11)$$

Since the rotor current is maintained at unity for maximum torque production, the stator flux magnitude in dc mode ψ_{sdc} is identical to the maximum torque in dc mode τ_{dc}, and (11) simplifies to

$$\omega_T = \frac{1}{\tau_{\mathrm{dc}}+1}. \quad (12)$$

Using (11) and (12), the minimum required rotor power electronics voltage rating is given by

$$v_{\mathrm{PE}} = \frac{\tau_{\mathrm{dc}}}{\tau_{\mathrm{dc}}+1}. \quad (13)$$

Using (10) in ac mode and (13), the associated maximum achievable shaft speed in ac mode with the minimum rotor power electronics voltage rating can be computed as

$$\omega_{\max} = \frac{2\tau_{\mathrm{dc}}+1}{\tau_{\mathrm{dc}}+1}. \quad (14)$$

Assuming no mechanical losses, the maximum shaft power is achieved at the maximum speed and is identical to (14) since the torque at maximum speed is unity. The minimum rotor power electronics power rating that enables wide-speed-range operation is identical to (13) since the rotor current is always maintained at unity. When the required dc mode torque is 75% to that of the rated torque, the minimum rotor power electronics rating can be 30% of maximum shaft power while operating on a speed range of 0–1.43 p.u. Equations (13) and (14) can be used to compute the ratio of $V_{\mathrm{PE}}/\omega_{\max}$, which is also the ratio of minimum rotor power electronics rating to maximum shaft power at unity maximum rotor current and maximum shaft torque. Fig. 3 shows the benefit and the design tradeoffs for the proposed drive architecture using (13) and (14).

The maximum speed requirement for the drive can be achieved in three ways. First, by choosing the ac supply frequency precisely in cases where system-level design is possible, e.g., a "blank slate" design for a ship or a train. Second, choosing and designing a DFM with a specific number of poles in cases where the ac supply frequency is fixed. Finally, if either of the above two is already constrained, the maximum speed will be set by the minimum voltage rating of the rotor power electronics. An increase in the maximum speed requirement will increase the voltage rating of the rotor power electronics.

To summarize, for proper utilization, the torque capability of the DFM must be equal to the required torque at high speed. Since in ac mode the stator flux is strictly determined by the ac supply voltage and frequency, the choice of high-speed torque requirement strongly influences the rotor power electronics current rating. The choice of low-speed-mode torque requirement strongly influences rotor power electronics voltage rating (since by fixing rotor current to be the same as in ac mode, the dc mode stator flux can be altered). The torque requirements significantly influence the transition speed, the maximum speed, and, of course, the required rotor power electronics power rating.

B. Drive Design for a Nonideal DFM

The presence of resistances, leakages, and finite magnetizing current in a practical DFM must be taken into account while minimizing the rotor power electronics rating such that the machine is operated within its rated capability. In practice, the stator and rotor current ratings might not be equal, and hence, the rated stator current is chosen as the base current for normalization, whereas the rated rotor current reflected to the stator is designated as I_r p.u. This section will review design considerations for a practical DFM propulsion drive. Specific examples will be illustrated using parameters from our

TABLE I
DFM PARAMETERS

Parameter	Actual	p.u
Stator resistance	3.575 Ω	0.1013
Rotor resistance (ref. to stator)	4.229 Ω	0.1199
Stator leakage inductance	9.6 mH	0.1024
Rotor leakage inductance (ref. to stator)	9.6 mH	0.1024
Mutual inductance	165 mH	1.7630
Stator current rating	5.09 A (peak)	1
Rotor current rating (ref. to stator) (I_r)	3.857 A (peak)	0.7576
Turns ratio (rotor to stator)	0.682	

experimental machine (1 hp, 220 V/150 V, 60 Hz, four pole, 1800 r/min) shown in Table I. The ac source is considered to be 220 V 60 Hz for this analysis. These parameters are not representative of a real ship propulsion motor.

The goal is to minimize the rotor power electronics requirements while the machine operates with a desired torque capability across the complete speed range within rated conditions. The sizing of the rotor power electronics starts with selecting the rotor power electronics current rating such that the candidate DFM is utilized to its maximum capability in ac mode. Once the current rating is determined, the dc mode stator flux is minimized to achieve the low-speed drive torque requirement. This directly impacts the rotor power electronics voltage rating by affecting the slope of the required rotor voltage, as highlighted in Fig. 2. A choice of dc mode stator flux also fixes the required dc supply voltage. Finally, the transition speed and the maximum speed are set to minimize the voltage rating and, therefore, the power rating of rotor power electronics. Additionally, the limits on the d- and q-axis currents are computed for both modes to ensure that the DFM operates within the rated limits of stator and rotor currents.

1) AC Mode: Choice of Rotor Power Electronics Current Rating: Due to the possibility of different current ratings in the stator and the rotor in a practical DFM, the rotor power electronics current rating must be chosen such that the machine stator and rotor current limits are not exceeded. The objective is to utilize the candidate DFM to its maximum torque capability in high-speed mode. Assume that the stator is connected to a stiff ac voltage source

$$v_{sd}^2 + v_{sq}^2 = 1. \tag{15}$$

Since r_s in a typical machine is small, (15) can be simplified using (1), (2), and (7) to compute the stator flux in ac mode, i.e.,

$$\psi_{\text{sac}} = 1 + \frac{r_s x_m}{x_s} i_{rq}. \tag{16}$$

The rotor current limit requires that

$$i_{rd}^2 + i_{rq}^2 \leq I_r^2. \tag{17}$$

The stator current limit necessitates

$$i_{sd}^2 + i_{sq}^2 \leq 1. \tag{18}$$

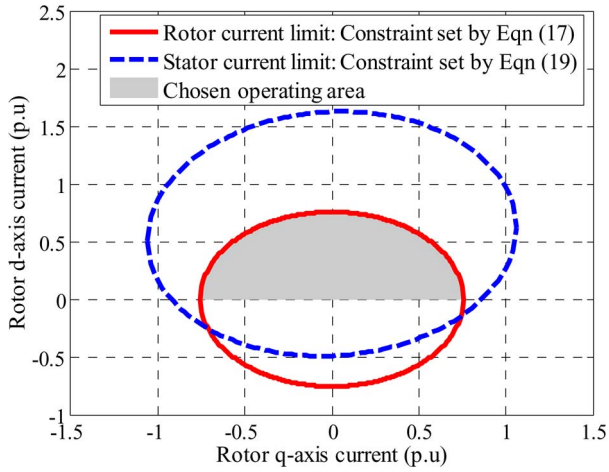

Fig. 4. AC mode: the DFM stator and rotor current ratings limit the maximum allowable rotor d- and q-axis currents, which set the rotor power electronics current rating.

Using (6) and (7), the stator currents can be substituted with rotor currents in (18), which results in

$$\left(\frac{\psi_{\text{sac}} - x_m i_{rd}}{x_s}\right)^2 + \left(-\frac{x_m i_{rq}}{x_s}\right)^2 \leq 1. \tag{19}$$

Constraints (17) and (19) are plotted in the $d-q$ rotor current plane, as shown in Fig. 4. The intersection area of the two constraints sets the safe operating current limits in ac mode. The maximum torque capability of the DFM is achieved when maximum negative q-axis current can be fed to the rotor of the DFM within the safe operating area. In the example DFM, the maximum torque capability is achieved when the rotor q-axis current is identical to the rotor current rating and the rotor d-axis current is zero. The rotor power electronics current rating, therefore, must be equal to the rotor current rating.

2) AC Mode: Determination of Maximum Torque Capability of the Candidate DFM: With the maximum q-axis rotor current that can be driven into the rotor being known, using (5) and (16), the maximum torque capability of the candidate DFM can be computed as

$$\tau_{\max} = \frac{x_m}{x_s}\left(1 - \frac{r_s x_m}{x_s} I_r\right) I_r. \tag{20}$$

If the torque requirement at high speed is smaller than the capability, the candidate DFM will be an oversized machine, left unutilized from the torque capability perspective. The "extra" capability may be utilized for reactive power control. If the torque requirement is larger than the capability, an alternate DFM design must be selected. Equations (5) and (16) are used to plot the maximum torque capability of the example DFM ($\tau_{\max} = 0.663$ p.u.) and the drooping behavior of the stator flux with increasing torque due to the resistances and leakages in the machine, as shown in Fig. 5.

3) AC Mode: Choice of Rotor D-Axis Current Limit: In ac mode, a secondary objective may be to achieve power factor control on the stator when connected to the ac source. For example, any extra or spare rotor inverter and DFM capability may be used achieve reactive power control of the ship microgrid.

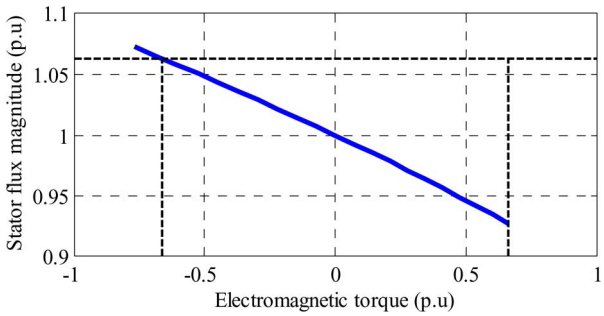

Fig. 5. AC mode: droop characteristic of the stator flux with torque due to presence of stator resistance and leakages for the example DFM.

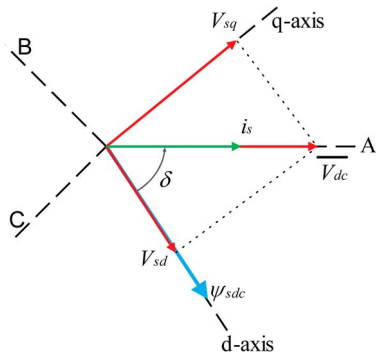

Fig. 6. DC mode: steady-state space vector diagram.

This is an exciting opportunity to allow the drive to assist with overall power system stability and an opportunity that may make the DFM VSD attractive in many other applications besides propulsion.

The limit of the rotor d-axis current rating, which affects stator power factor, can be obtained from the stator and rotor current ratings. From (16), (17), and (19), for a particular q-axis rotor current, the upper limit is

$$i_{rd}|_{\max} \le \text{Min}\left(\sqrt{I_r^2 - i_{rq}^2}, \left(1 + \frac{r_s x_m}{x_s} i_{rq} + x_s\sqrt{1 - \left(\frac{x_m i_{rq}}{x_s}\right)^2}\right) \Big/ x_m\right) \quad (21)$$

whereas the lower limit is

$$i_{rd}|_{\min} \ge \text{Max}\left(-\sqrt{I_r^2 - i_{rq}^2}, \left(1 + \frac{r_s x_m}{x_s} i_{rq} - x_s\sqrt{1 - \left(\frac{x_m i_{rq}}{x_s}\right)^2}\right) \Big/ x_m\right). \quad (22)$$

For the parameters of the example machine, the stator current limit imposes a minimum d-axis rotor current of negative value, which does not provide any benefit in ac mode unless the DFM has to operate as a reactive power sink. The minimum d-axis rotor current is, therefore, chosen to be zero. The chosen operating area for the rotor current is shown in Fig. 4.

4) DC Mode: Choice of DC Mode Stator Flux and Source Voltage: The design process continues with selection of dc mode stator flux and dc source voltage based on the required torque in dc mode. This directly influences the to-be-selected rotor power electronics voltage rating by affecting the slope of the required rotor voltage curve relative to the operating speed in dc mode. As an example, the required torque in dc mode is chosen as 75% of the ac mode torque (equivalent to 0.498 p.u. for the example DFM). Assuming that the positive dc supply is connected to the stator A phase, whereas the negative is connected to the B and C phases, Fig. 6 shows the space vectors of the stator flux and voltage. Denoting the angle between the stator voltage vector and the stator flux vector as δ, the electromagnetic torque in dc mode can be expressed using (5) and (7) as

$$\tau_{\text{dc}} = i_s \psi_{\text{sdc}} \sin\delta \quad (23)$$

where $i_s = v_{\text{dc}}/r_s$.

The required torque in dc mode should be achieved at minimum stator flux magnitude, which implies that the stator current and the angle δ need to be maximized within allowable limits. The upper bound on δ for steady operation is 90°, and the upper bound on the stator current is determined by two constraints. First, the stator current rating of the machine must not be exceeded. Second, the reflected rotor current must not exceed the power electronics and the DFM current ratings both in the steady state and during transients. These bounds can be simultaneously mapped on a $\delta - i_s$ plane, as shown in Fig. 7. To keep the machine stator current within its RMS rating (since the stator current is dc)

$$i_s \le \frac{1}{\sqrt{2}}. \quad (24)$$

Using (7) and (23)

$$i_{rq} = -\frac{x_s}{x_m} i_s \sin\delta. \quad (25)$$

Similarly, (6) can be rearranged in dc mode, resulting in

$$i_{rd} = \frac{\psi_{\text{sdc}}}{x_m} - \frac{x_s}{x_m} i_s \cos\delta. \quad (26)$$

At steady state, the stator voltage vector, current vector, and A-phase axis coincide, as shown in Fig. 6. Therefore, to keep the rotor current within its rated limit at steady state, (23), (25), and (26) are combined to obtain

$$i_r = \sqrt{\left(-\frac{x_s}{x_m} i_s \sin\delta\right)^2 + \left(\frac{\tau_{\text{dc}}}{x_m i_s \sin\delta} - \frac{x_s}{x_m} i_s \cos\delta\right)^2} \le I_r. \quad (27)$$

The rotor current must also be within its rated limit during transient torque demand. A step change in torque demand of τ_{dc} from zero can be considered as the worst case in this regard. The DFM model described by (1) and (2) is extended to incorporate the time-derivative terms, resulting in

$$v_{sd} = r_s i_{sd} + \frac{1}{\omega_B}\frac{d\psi_s}{dt}$$
$$v_{sq} = r_s i_{sq} + \psi_{\text{sdc}}\frac{1}{\omega_B}\frac{d\delta}{dt}. \quad (28)$$

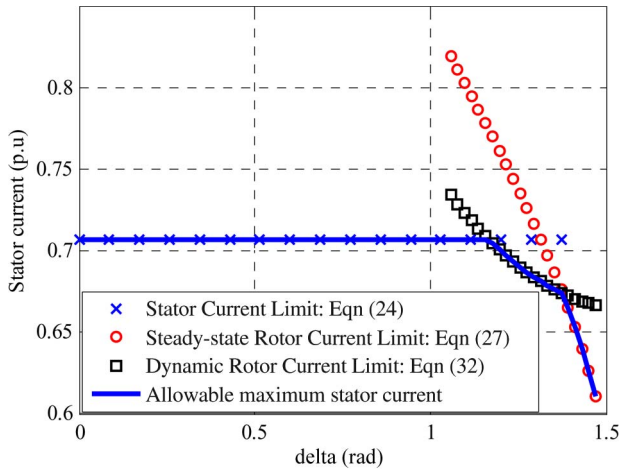

Fig. 7. DC mode: bounds on allowable stator current due to the stator and rotor current limits with respect to the angle δ.

With zero torque demand initially, the angle δ is zero, implying that the stator flux and dc source voltage vectors are aligned along the stator A-phase axis. The stator flux is maintained constant using rotor d-axis current, from (28)

$$i_{sd} = \frac{v_{\rm dc}}{r_s} = i_s. \tag{29}$$

Using (6) and (29), the required rotor d-axis current to maintain the stator flux constant is obtained as

$$i_{rd} = \frac{\psi_{\rm sdc}}{x_m} - \frac{x_s}{x_m} i_s. \tag{30}$$

Equation (28) also suggests that the angle δ does not instantaneously change with the change in torque demand. A step demand in torque of $\tau_{\rm dc}$ will require a q-axis rotor current from (5) as

$$i_{rq} = -\frac{x_s \tau_{\rm dc}}{x_m \psi_{\rm sdc}}. \tag{31}$$

Therefore, using (23) in (30) and (31), the dynamic limit on the d- and q-axis rotor currents can be formulated as

$$i_r = \sqrt{\left(-\frac{x_s}{x_m} i_s \sin\delta\right)^2 + \left(\frac{\tau_{\rm dc}}{x_m i_s \sin\delta} - \frac{x_s}{x_m} i_s\right)^2} \le I_r. \tag{32}$$

Equations (24), (27), and (32) set the allowable stator current limit for the required dc mode torque, as shown in Fig. 7. The minimum dc mode stator flux can be computed from (23) as

$$\min_{i_s,\delta} \ \psi_{\rm sdc} = \frac{\tau_{\rm dc}}{i_s \sin\delta}$$

Subject to :

$$\delta < 90^\circ$$

$$i_s(\delta) \text{ is bounded by (24), (27), (32).} \tag{33}$$

The minimum stator flux is obtained at the angle $\delta_{\max}$, as shown in Fig. 8. The minimum stator flux obtained for the example DFM is 0.75 p.u. The angle $\delta_{\max}$ and the obtained minimum

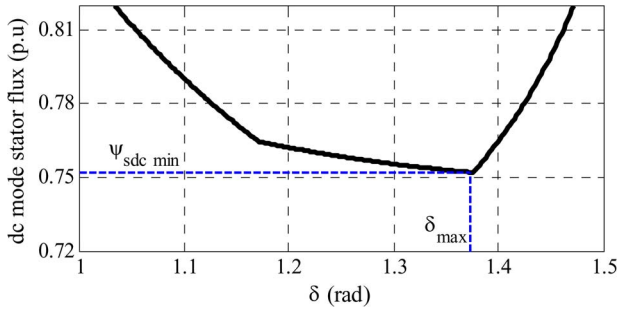

Fig. 8. Maximum operating δ is chosen such that dc mode stator flux is minimized that reduces required rotor power electronics voltage rating.

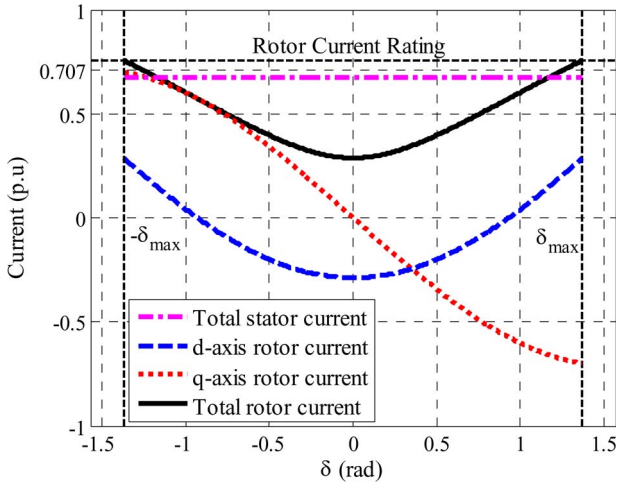

Fig. 9. DC mode: the stator and rotor currents of the DFM are within the rated value for all operating drive torque and with minimum stator flux magnitude.

stator flux magnitude can be used to compute the required dc source voltage using (23).

Fig. 9 shows that the chosen dc mode stator flux magnitude achieves the drive torque requirement within the allowable bounds on the DFM current ratings and the allowable $\delta_{\max}$. The rotor d- and q-axis current limits in dc mode are different than in ac mode. This must be appropriately accounted in the drive controller.

5) Rotor Power Electronics Voltage Rating: Computation of Transition Speed and Maximum Speed: With the minimized stator flux in dc mode and the rotor current in ac mode, (1)–(9) can be used to compute the rotor voltage requirement for the entire operating speed range. This is plotted in Fig. 10. Comparing with the rotor voltage requirement of the ideal DFM in Fig. 2, there are notable differences due to presence of nonidealities in the DFM.

Not only that nonzero rotor voltages are required at zero and unity speeds but also the magnitude depends on the polarity of the demanded electromagnetic torque. This implies a different rotor voltage requirement during acceleration and deceleration for the drive load. To minimize required rotor voltage to operate the drive under all operating conditions, a mode transition speed is chosen such that required rotor voltage in dc mode for maximum positive torque is equal to that in ac mode for maximum negative torque. The maximum operating speed of the drive can be obtained based on the chosen minimum rotor voltage and

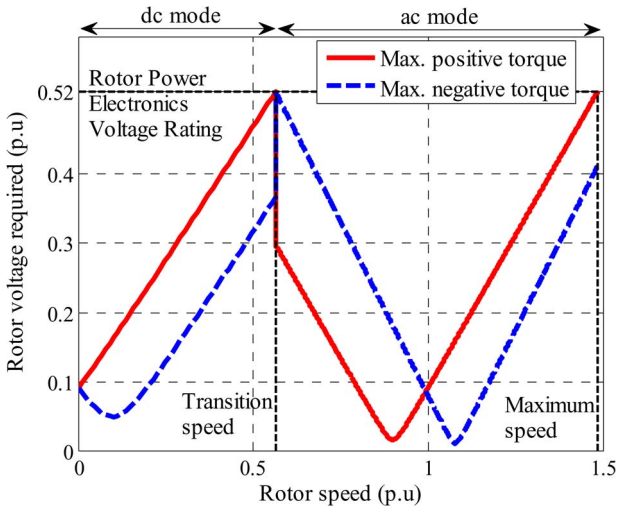

Fig. 10. Example DFM: 0.52 p.u. rotor power electronics voltage rating can enable operation within 0–1.49 p.u. speed.

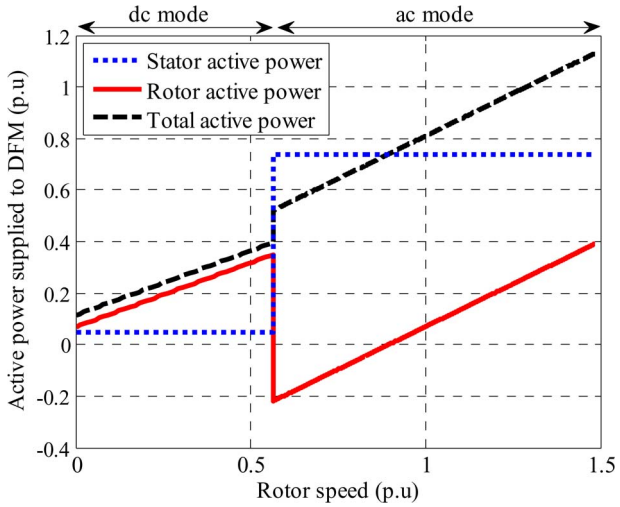

Fig. 11. Example DFM: one-third rotor power electronics power rating can control the net active power flowing to the DFM while operating on a speed range of 0–1.49 p.u.

voltage requirement in ac mode for maximum positive torque. For the example DFM, the required rotor power electronics voltage rating is 0.52 p.u. while operating on a speed range of 0–1.49 p.u. The sharing of total active power between the stator and the rotor for the nonideal DFM is shown in Fig. 11. The maximum power being handled by the rotor power electronics is 0.39 p.u., whereas the maximum total active power fed to the DFM is 1.13 p.u. Therefore, a rotor power electronics of one-third power rating can be used to control the example DFM over the complete speed range. Depending on the efficiency of the DFM and the mechanical drive train, the net output shaft power is determined.

Fig. 12 shows the steady-state torque-speed capability of the example DFM with the proposed drive architecture. A typical propulsion load torque is also shown, which is proportional to the square of rotor speed and matches the maximum torque capability of the DFM at maximum speed.

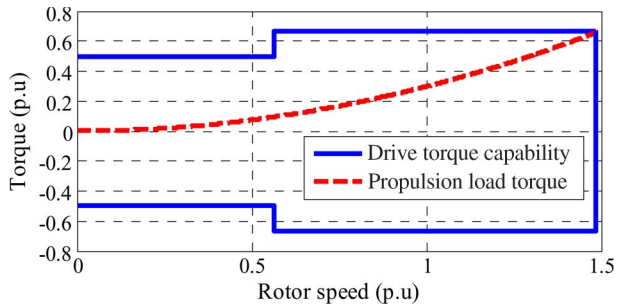

Fig. 12. Designed drive torque-speed capability of the example DFM using the proposed architecture with a typical propulsion load torque.

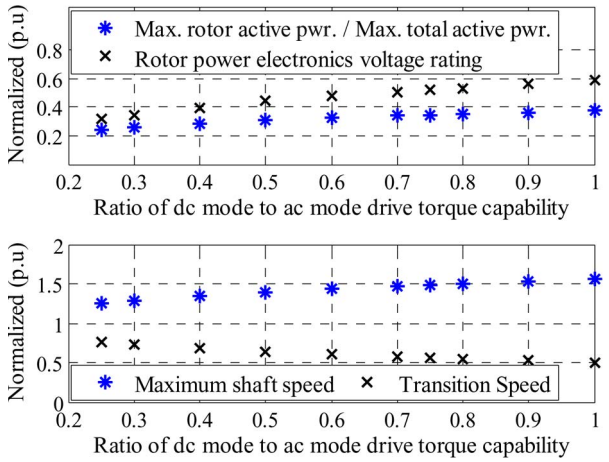

Fig. 13. Example DFM: effect of different low-speed torque requirements on the rotor power electronics power rating and voltage rating (top) and on the transition speed and maximum shaft speed (bottom).

In general, the procedure can be used for designing the switched DFM drive with different drive torque capability requirements in low speed. Fig. 13 shows the effect of different dc mode torque capability requirements on the rotor converter size and operating drive speed for the example DFM. The effect is similar to an ideal DFM, as shown in Fig. 3.

C. Dynamic Analysis: Mode Transition Consideration on Drive Design

A dynamic analysis of the proposed drive is required to ensure that the designed rotor power electronics has sufficient capability to drive the machine through the transition between modes without undesirable shaft and power disturbances. In ac mode, the stator flux is set by the ac source voltage and frequency, whereas in dc mode, the stator flux magnitude is controllable through the stator flux controller [9]. The stator flux magnitude, therefore, transitions from a controllable state to an uncontrollable state in a dc-to-ac mode changeover. Assuming that the current controller bandwidth is sufficiently high, the dynamics involved in the dc-to-ac mode transition can be simplified with two state variables: the stator flux magnitude and the angle between the stator flux and the stator voltage. In ac mode

$$v_{sd} = \cos\delta$$
$$v_{sq} = \sin\delta. \tag{34}$$

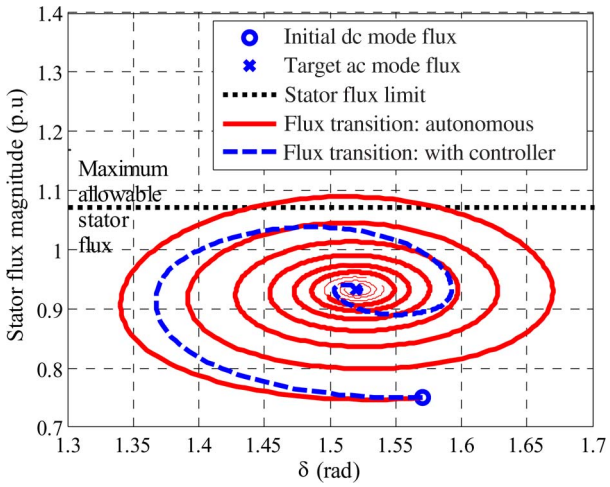

Fig. 14. Phase plane plot: stator flux trajectory for a dc-to-ac mode transition with and without flux transition controller.

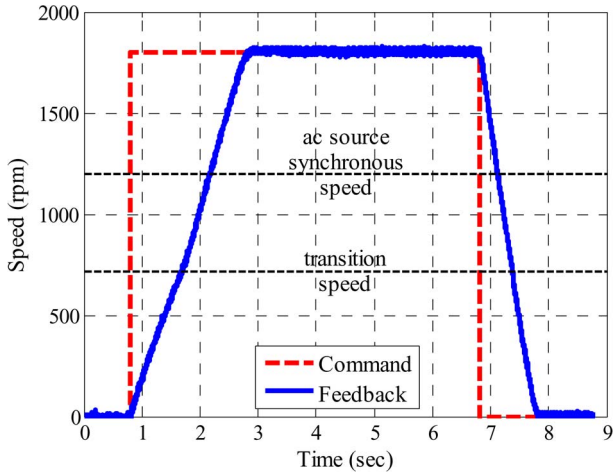

Fig. 15. Experimental result: speed response of the switched DFM drive for a step command in speed.

Using (6), (7), (28), and (34), the stator flux transient dynamics during dc-to-ac mode transition are governed by

$$\frac{1}{\omega_B}\frac{d}{dt}\psi_s = \cos\delta - \frac{r_s}{x_s}\psi_s + \frac{r_s x_m}{x_s} i_{rd}$$
$$\frac{1}{\omega_B}\frac{d\delta}{dt} = 1 - \frac{1}{\psi_s}\sin\delta - \frac{1}{\psi_s}\frac{r_s x_m}{x_s} i_{rq}. \quad (35)$$

This model is equivalent to the widely used DFM model [10] for stability analysis of grid-connected doubly fed induction generator. The initial value of the stator flux magnitude is obtained from operating level in dc mode, whereas the initial value for the angle is obtained from the switching instant from dc mode to ac mode as determined by the synchronizer [9].

For the autonomous response of the DFM during a dc-to-ac mode transition, the d-axis rotor current is set to zero, and the q-axis rotor current is commanded based on the required torque. The autonomous response of the nonlinear model described by (35) is shown in the phase plane plot in Fig. 14. Although the transition is stable, the stator flux swings higher than the desired level. The maximum stator flux that can be handled by the rotor inverter based on the steady-state design, as shown in Fig. 5, is marked in Fig. 14. This can make the rotor power electronics voltage limited, and the DFM will experience undesirable torque and power disturbances. Since the q-axis current is used to control the torque of the DFM under all operating modes, the d-axis current can be used to suppress the stator flux swing during the transition. In the example DFM, the stator flux transition controller [9] ensures that, during dc-to-ac mode transition, the stator flux magnitude remains within the design limit.

III. Experimental Results

Experiments have been performed on the example DFM to illustrate sizing benefit of the rotor power electronics for the proposed DFM drive while the DFM is operated within its rated condition. Two Texas Instruments High Voltage Motor Control and PFC Developer's Kits, which are named Kit-I and Kit-II, are used for this purpose. Kit-I is programmed to emulate either an ac source of 134 V 40 Hz or a dc source of 20 V. The choice of the ac source voltage ensures that the off-the-shelf DFM remains within the rated operating speed of 1800 r/min. The rotor is connected to Kit-II. The complete controller is programmed in TMS320F28035 placed in Kit-II. A mode switching command from Kit-II switches the excitation of Kit-I. Although this would not be the case in an actual implementation where a transfer switch will connect the stator between the dc and ac sources, this setup is chosen to validate the rotor power converter sizing benefit.

The DFM drive is subjected to a step command in a speed of 1.5 p.u. Once steady state is reached, zero speed is commanded, as shown in Fig. 15. A unique controller [9] ensures a smooth operation of the proposed drive in and through the two modes. The internal relevant variables during the experiment are recorded from the digital-to-analog converter output of Kit-II. The measured voltages are additionally corrected for device and brush drops.

The measured rotor voltage magnitude command, reflected to the stator, is plotted with respect to the measured speed to illustrate the reduction in requirement of the rotor voltage power electronics while operating on the complete speed range, as shown in Fig. 16(a) and (b) (during acceleration and deceleration, respectively). The experimental results resemble the simulation result obtained from a dynamic model developed in MATLAB. As expected from the design analysis, the voltage requirement profile is different during acceleration and deceleration. The maximum required rotor voltage is 0.45 p.u. while operating on a speed range of 0–1.5 p.u. The sharing of the total active power being fed to the DFM is shown in Fig. 16(c) and (d) (during acceleration and deceleration, respectively). While the total active power handled by the DFM reaches 900 W at full speed, the rotor power electronics handle only 300 W across the complete speed range, resulting in a rotor power electronics sizing of one third of the total power rating. The actual transition speed depends on the correct instant of transition as governed by the synchronizer [9] for a "bumpless" mode transition. Additionally, a hysteresis comparator between the measured speed and the designed transition speed ensures a chatter-free mode transition. This leads to a slightly different

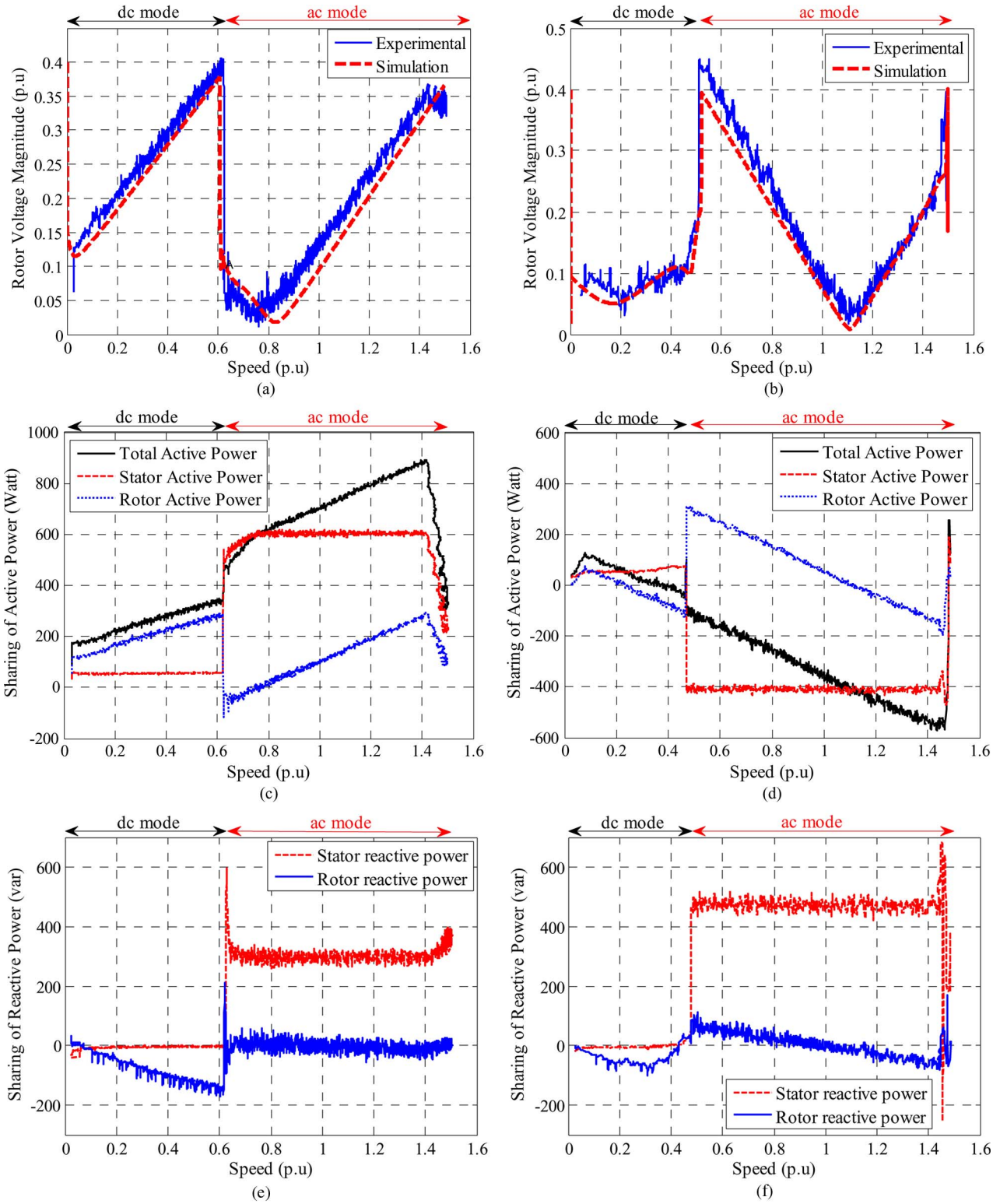

Fig. 16. Experimental result: performance variable measured during the step response of the DFM. The ac synchronous speed is set at 1200 r/min (corresponding to 1 p.u.), whereas the mode transition speed is set at 720 r/min (corresponding to 0.6 p.u.). (a) Measured rotor power electronics voltage command during acceleration (full positive torque) versus shaft speed. (b) Measured rotor power electronics voltage command during deceleration (full negative torque) versus shaft speed. (c) Sharing of the active power fed to the DFM between the stator and the rotor during acceleration. (d) Sharing of the active power fed to the DFM during deceleration. (e) Sharing of the reactive power fed to the DFM between the stator and the rotor during acceleration. (f) Sharing of the reactive power fed to the DFM between the stator and the rotor during deceleration.

transition speed during acceleration and deceleration. The sharing of the reactive power is shown in Fig. 16(e) and (f) (during acceleration and deceleration, respectively). In dc mode, the rotor power electronics supplies the reactive power to the DFM entirely. In ac mode, the reactive power can be shared between stator and rotor depending on the designed extra capability of

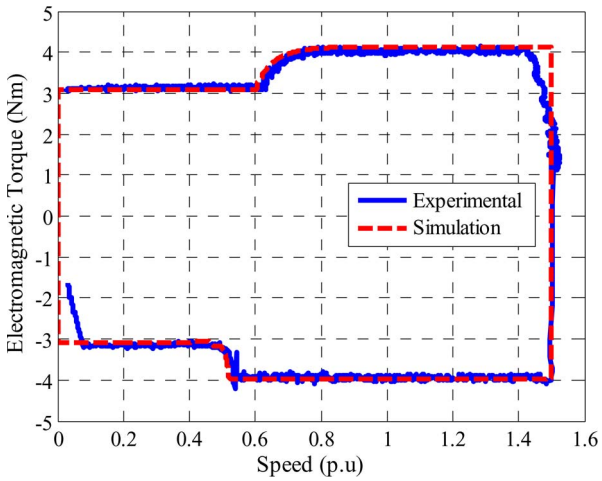

Fig. 17. Experimental result: drive torque-speed capability. Low-speed mode has 75% torque capability to that of high-speed mode as designed.

the rotor power electronics. In Fig. 16(e), the entire reactive power in ac mode is supplied by the stator by commanding zero d-axis rotor current. A step demand in reactive power from the ac source during the dc-to-ac mode transition can be nullified by proper control of the front-end converter to be placed in an actual system. In Fig. 17(f), during deceleration, rotor power electronics partly share the reactive power requirement of the DFM as programmed by commanding rotor d-axis current.

The electromagnetic torque developed by the DFM drive during the acceleration and deceleration process is plotted in Fig. 17. The dc mode torque limit is set as 75% to that of the ac mode torque limit as demonstrated in the design process. The result is compared against the dynamic model simulation in MATLAB. As the actual speed of the DFM is near the commanded speed, the speed controller reduces the electromagnetic torque demand. This can be seen beyond the speed of 1.44 p.u. in positive torque region required during acceleration and 0.06 p.u. in negative torque region during deceleration.

IV. Conclusion

This paper has discussed a design process for a switched DFM drive. Two mode operations permit full-speed-range VSD when an ac utility is available. While ac-mode operation impacts the current rating, dc-mode operation impacts the voltage rating of the rotor power electronics. Given a DFM and torque requirements, the rotor power electronics can be minimized with proper choice of transition speed between modes and maximum desirable speed. Although an exemplary design has been shown with a propulsion load torque profile, the design can be iterated for other desirable load torque profiles such as traction, which require higher torque in low speed and lower torque in high speed. Using similar drive architecture but designing for higher dc mode torque compared with ac mode torque can satisfy the traction torque requirement. The drive architecture also provides flexibility of introducing a third mode, i.e., "high-speed dc" mode, when the ac mode can be switched back to dc mode but with lower effective stator flux, allowing a field weakening operation. The design approach described can be also used to design switched DFM drive with shorted stator in low-speed mode. Furthermore, the drive shown in this paper operates in two quadrants, i.e., with positive speed and bipolar torque. The drive can be easily operated in negative speed ranges in dc mode with no further modification. With an added phase changing switch for the ac source, the drive can be operated in all the four quadrants of the speed-torque region with symmetrical capability.

References

[1] F. Blaabjerg, M. Liserre, and K. Ma, "Power electronics converters for wind turbine systems," *IEEE Trans. Ind. Appl.*, vol. 48, no. 2, pp. 708–719, Mar./Apr. 2012.

[2] H. Akagi and H. Sato, "Control and performance of a doubly-fed induction machine intended for a flywheel energy storage system," *IEEE Trans. Power Electron.*, vol. 17, no. 1, pp. 109–116, Jan. 2002.

[3] L. Morel, H. Godfroid, A. Mirzaian, and J.-M. Kauffmann, "Double-fed induction machine: Converter optimisation and field oriented control without position sensor," *IEE Proc.-Elect. Power Appl.*, vol. 145, no. 4, pp. 360–368, Jul. 1998.

[4] F. Bonnet, L. Lowinsky, M. Pietrzak-David, and P.-E. Vidal, "Doubly fed induction machine speed drive for hydro-electric power station," in *Proc. Eur. Conf. Power Electron. Appl.*, Sep. 2–5, 2007, pp. 1–9.

[5] S. B. Leeb *et al.*, "How much dc power is necessary?" *Nav. Eng. J.*, vol. 122, no. 2, pp. 79–92, Jun. 2010.

[6] X. Yuan, J. Chai, and Y. Li, "A converter-based starting method and speed control of doubly fed induction machine with centrifugal loads," *IEEE Trans. Ind. Appl.*, vol. 47, no. 3, pp. 1409–1418, May/Jun. 2011.

[7] S. P. Verma, "Noise and vibrations of electrical machines and drives; their production and means of reduction," in *Proc. Int. Conf. Power Electron. Drives Energy Syst. Ind. Growth*, Jan. 8–11, 1996, vol. 2, pp. 1031–1037.

[8] R. Fischer and K. Yankaskas, "Noise control on ships-enabling technologies," Office Naval Res., Arlington, VA, USA, Tech. Rep., 2011.

[9] A. Banerjee, M. S. Tomovich, S. B. Leeb, and J. L. Kirtley, "Control architecture for a switched doubly-fed machine propulsion drive," *IEEE Trans. Ind. Appl.*, to be published.

[10] G. D. Marques and D. M. Sousa, "Stator flux active damping methods for field-oriented doubly fed induction generator," *IEEE Trans. Energy Convers.*, vol. 27, no. 3, pp. 799–806, Sep. 2012.

Arijit Banerjee (S'12) received the B.E. degree in electrical engineering from Bengal Engineering and Science University, Howrah, India, in 2005 and the M.Tech. degree in electrical engineering from the Indian Institute of Technology Kharagpur, Kharagpur, India, in 2007. He is currently working toward the Ph.D. degree at Massachusetts Institute of Technology, Cambridge, MA, USA.

During 2006–2007, he was a Visiting Student with the Institute for Power Electronics and Control of Drives, Technische Universität Darmstadt, Darmstadt, Germany, under a German Academic Exchange Service (DAAD) Fellowship. From 2007 to 2011, he was with the Power Conversion Systems Group, General Electric Global Research Centre, Bangalore, India, where he was working on monitoring and diagnostics of electromechanical systems using electrical signatures. In 2011, he joined the Laboratory for Electromagnetic and Electronic Systems, Massachusetts Institute of Technology. He is the holder of ten issued patents and several patent applications. His research interests include analysis, design, control, and diagnostics of electromechanical systems.

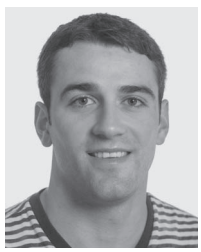

Michael S. Tomovich (S'12) received the B.S. degree in electrical and computer engineering in 2011 from Carnegie Mellon University, Pittsburgh, PA, USA, where he worked with Team Astrobotic in pursuit of the Google Lunar X Prize, and the S.M. degree in electrical engineering and computer science in 2014 from Massachusetts Institute of Technology (MIT), Cambridge, MA, USA, where his research was in power electronics and motor control.

His research interests include embedded systems, power electronics, and entrepreneurship.

Mr. Tomovich was a member of the MIT Global Founders' Skills Accelerator in the summer of 2013.

Steven B. Leeb (F'07) received the Ph.D. degree from Massachusetts Institute of Technology (MIT), Cambridge, MA, USA, in 1993.

He served as a Commissioned Officer in the U.S. Air Force Reserve. He holds a joint appointment in the Department of Mechanical Engineering, MIT, where he is currently a MacVicar Fellow and a Professor of electrical engineering and computer science in the Laboratory for Electromagnetic and Electronic Systems and has been a member of the faculty of the Department of Electrical Engineering and Computer Science since 1993. In his capacity as a Professor at MIT, he is concerned with the design, development, and maintenance processes for all kinds of machinery with electrical actuators, sensors, or power electronic drives. He has authored or coauthored over 80 publications. He is the holder of 13 U.S. patents in the fields of electromechanics and power electronics.

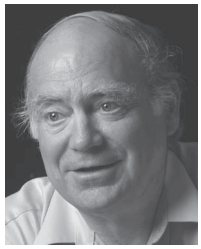

James L. Kirtley Jr. (LF'91) received the Bachelor's and Ph.D. degrees from Massachusetts Institute of Technology (MIT), Cambridge, MA, USA, in 1971.

He was an Electrical Engineer in the Large Steam Turbine Generator Department with General Electric and the Vice President and General Manager of the Tech Center and a Chief Scientist and a Director with Satcon Technology Corporation. He was a Gastdozent with the Swiss Federal Institute of Technology. He is currently a Professor of electrical engineering with MIT. He is a specialist in electric machinery and electric power systems.

Dr. Kirtley is a member of the Editorial Board of *Electric Power Components and Systems*. From 1998 to 2006, he served as the Editor-in-Chief of the IEEE TRANSACTIONS ON ENERGY CONVERSION, where he continues to serve as an Editor. He was a recipient of the IEEE Third Millennium Medal in 2000 and the Nikola Tesla Prize in 2002. He was elected to the U.S. National Academy of Engineering in 2007. He is a Registered Professional Engineer in Massachusetts.